New Pyrimido-Indole Compound CD-160130 Preferentially Inhibits the K_V11.1B Isoform and Produces Antileukemic Effects without Cardiotoxicity

Luca Gasparoli, Massimo D'Amico, Marika Masselli, Serena Pillozzi, Rachel Caves, Rawan Khuwaileh, Wolfgang Tiedke, Kenneth Mugridge, Alessandro Pratesi, John S. Mitcheson, Giuseppe Basso, Andrea Becchetti, and Annarosa Arcangeli

Department of Experimental and Clinical Medicine, University of Florence, Florence, Italy (L.G., S.P., A.A.); Department of Chemistry "Ugo Schiff," University of Florence, Florence, Italy (M.M., A.P.); DI.V.A.L. Toscana srl, Sesto Fiorentino, Italy (M.D.A., M.M.); Department of Cell Physiology and Pharmacology, University of Leicester, Leicester, United Kingdom (R.C., R.K., J.S.M.); BlackSwan Pharma GmbH, Leipzig, Germany (W.T., K.M.); Oncohematology Laboratory, Department of Woman and Child Health, University of Padova, Padova, Italy (G.B.); and Department of Biotechnologies and Biosciences, University of Milano-Bicocca, Milan, Italy (A.B.)

ABSTRACT

K_V11.1 (hERG1) channels are often overexpressed in human cancers. In leukemias, K_V11.1 regulates pro-survival signals that promote resistance to chemotherapy, raising the possibility that inhibitors of K_V11.1 could be therapeutically beneficial. However, because of the role of K_V11.1 in cardiac repolarization, blocking these channels may cause cardiac arrhythmias. We show that CD-160130, a novel pyrimido-indole compound, blocks K_V11.1 channels with a higher efficacy for the K_V11.1 isoform B, in which the IC_{50} (1.8 *m*M) was approximately 10-fold lower than observed in K_V11.1 isoform A. At this concentration, CD-160130 also had minor effects on K_{ir}2.1, K_V 1.3, K_V1.5, and K_{Ca}3.1. In vitro, CD-160130 induced leukemia cell apoptosis, and could overcome bone marrow mesenchymal stromal cell (MSC)-induced chemoresistance. This effect was caused by interference with the survival signaling pathways triggered by MSCs. In vivo, CD-160130 produced an antileukemic activity, stronger than that caused by cytarabine. Consistent with its atypical target specificity, CD-160130 did not bind to the main binding site of the arrhythmogenic K_V11.1 blockers (the Phe656 pore residue). Importantly, in guinea pigs CD-160130 produced neither alteration of the cardiac action potential shape in dissociated cardiomyocytes nor any lengthening of the QT interval in vivo. Moreover, CD-160130 had no myelotoxicity on human bone marrow–derived cells. Therefore, CD-160130 is a promising first-in-class compound to attempt oncologic therapy without cardiotoxicity, based on targeting K_V11.1. Because leukemia and cardiac cells tend to express different ratios of the A and B K_V11.1 isoforms, the pharmacological properties of CD-160130 may depend, at least in part, on isoform specificity.

Introduction

K_V11.1 (or hERG1), encoded by *KCNH2* or *hERG1* (Sanguinetti et al., 1995; Trudeau et al., 1995) is the pore-forming subunit of the rapid delayed rectifying K^1 current, which is a major regulator of action potential (AP) repolarization in the human cardiac ventricle (Sanguinetti and Tristani-Firouzi, 2006). K_V11.1 displays peculiar biophysical properties, which enable it to contribute to shaping the repolarization phase of the AP (Spector et al., 1996). Defective K_V11.1 can slow ventricular repolarization, thus predisposing certain individuals to long QT syndrome, a prolongation of the ECG QT interval (Tseng, 2001). Long QT syndrome can lead to arrhythmias, particularly to torsade de pointes (Viskin, 1999; De Bruin et al., 2005). Thus, pharmaceutical companies adopt an early screening policy to test the effects of any newly developed compound on K_V11.1 currents (Sanguinetti and Mitcheson, 2005). Such screening is mandatory for approval for clinical use.

Ample evidence shows that K_V11.1 channels are often aberrantly expressed in solid human cancers (Arcangeli, 2005) as well as in leukemias (Pillozzi et al., 2002, 2007; Arcangeli et al., 2012). K_V11.1 controls different aspects of cell malignancy, from proliferation and survival, to transendothelial

This work was supported by Associazione Italiana per la Ricerca sul Cancro (AIRC); Associazione Genitori Noi per Voi to AA; DI.V.A.L. Toscana srl to M.M.; University of Milano-Bicocca (FAR) to A.B. and British Heart Foundation project grant to J.S.M.

The authors declare no conflict of interests.

L.G., M.D.A., M.M., A.B. and A.A. contributed equally to this work.

ABBREVIATIONS: ALL, acute lymphoid leukemia; AML, acute myeloid leukemia; AP, action potential; BM, bone marrow; cAP, cardiac action potential; CFU, colony forming unit; CLL, chronic lymphoid leukemia; DMSO, dimethylsulfoxide; ECG, electrocardiografy; HEK 293, Human Embryonic Kidney 293 cells; MFI, mean fluorescence intensity; MSC, mesenchymal stromal cell; PBMNC, peripheral blood mononuclear cell; PDE-4, phosphodiesterase-4; siRNA, small interfering RNA; V_H, holding potential.

migration and bloodstream invasion (Arcangeli et al., 2012). Furthermore, in acute lymphoid leukemia (ALL), the $K_V11.1$ function is necessary for the development of tumor resistance to chemotherapy (Pillozzi et al., 2011), as blocking $K_V11.1$ decreases tumor growth in mice xenografted with leukemic cells, and in particular with chemoresistant cells (Pillozzi et al., 2011). ALL cells express a plasma membrane complex constituted by $K_V11.1$, the $\beta1$ integrin subunit and the SDF-1α receptor CXCR4. This complex mediates the protection from chemotherapeutics conferred to ALL by mesenchymal stromal cells (MSCs) (Pillozzi et al., 2011). Classic $K_V11.1$ blockers impede complex formation and overcome chemoresistance in vivo and in vitro.

The aforementioned evidence and the observation that $K_V11.1$ regulates proliferation and apoptosis in other tumors (Arcangeli, 2005; Arcangeli et al., 2009; Jehle et al., 2011) indicate $K_V11.1$ as a potential target for antineoplastic therapy, provided that one can avoid cardiotoxic effects. A possible solution is suggested by the observation that *KCNH2* expresses at least two alternative transcripts, *KCNH2a* and *KCNH2b*, coding for $K_V11.1A$ and $K_V11.1B$ proteins, respectively. $K_V11.1B$ presents a shortened and distinct N terminus, constituted by 34 amino acid residues. This peculiar domain determines the faster deactivation gating typically observed in $K_V11.1B$ (Lees-Miller et al., 1997; Morais Cabral et al., 1998). The relative abundance of these isoforms determines the kinetic properties of the rapid delayed rectifying K^1 current (Pond et al., 2000; Jones et al., 2004; Sale et al., 2008; Larsen and Olesen, 2010). In cardiac myocytes both isoforms contribute to the rapid delayed rectifying K^1 current although $K_V11.1A$ tends to predominate (Pond et al., 2000; Jones et al., 2004; Sale et al., 2008; Larsen and Olesen, 2010). On the contrary, leukemias mainly express $K_V11.1B$ (Crociani et al., 2003; Pillozzi et al., 2007), and overexpression of the *KCNH2b* transcript in pediatric T-ALL identifies a patients' subgroup with a worse prognosis (Pillozzi et al., 2014). Therefore, one possibility of circumventing the risk of developing torsade de pointes in patients treated with $K_V11.1$ blockers would be to selectively inhibit $K_V11.1B$, the leukemia-specific channel isoform (Arcangeli et al., 2012).

CD-160130 is a novel pyrimido-indole drug with a weak phosphodiesterase-4 (PDE-4) inhibiting activity. Preliminary results suggest that this compound induces apoptosis of chronic lymphoid leukemia (CLL) cells (Weinberg et al., 2007). We have determined the effects of CD-160130 on the $K_V11.1$ isoforms by using patch-clamp techniques. Additionally, the antineoplastic effects of CD-160130 on several human leukemia cell lines and primary samples have been examined by assessing its cell killing and proapoptotic properties. Finally, we evaluated the antileukemic activity of CD-160130 in vivo in an acute myeloid leukemia (AML) mouse model, and tested its effects in guinea pigs, either on the AP of acutely isolated cardiac ventricular myocytes or on ECG parameters in vivo.

Materials and Methods

Cell Culture and Treatment

Cell Culture and Transfection. Acute leukemia cell lines and MSCs were cultured as previously described (Pillozzi et al., 2007, 2011). MSC co-cultures were established as in Pillozzi et al. (2011). The MEC1 cell line was maintained in Iscove's modified Dulbecco's medium with 5% heat-inactivated fetal bovine serum. Human Embryonic Kidney 293 (HEK 293) cells were cultured and transfected with different vectors (see Supplemental Material) as previously reported (Crociani et al., 2013). Chinese hamster ovary cell lines were cultured and transfected as in Guasti et al. (2008). L 929 cells were cultured and transfected as in Zimin et al. (2010), except that LipofectAMINE 2000 (Invitrogen, Carlsbad, CA) was used for transfection. For electrophysiology, the adherent cells were harvested using 0.25% trypsin/EDTA (Invitrogen).

Leukemic B and Peripheral Blood Mononuclear Cell (PBMNC) Isolation. Leukemic B cells were purified using the RosetteSep human B cell enrichment cocktail (STEMCELL Technologies, Vancouver, Canada) and the Ficoll-Hypaque (Pharmacia, Uppsala, Sweden) density gradient centrifugation. Cells were resuspended as in Levesque et al. (Levesque et al., 2001). PBMNCs were isolated from buffy coat preparation of two independent healthy donors, using the Ficoll-Hypaque gradient centrifugation. Mononuclear cells were recovered at the interphase, washed, counted, and then used in the viability experiments.

Clonogenic Assay

Bone marrow (BM) aspirates from patients in complete remission were obtained from the Oncohematology Laboratory of the Department of Woman and Child Health, University of Padova (under informed consent). BM cells were cultured on MethoCult GF H4034 (STEMCELL Technologies), designed to support growth of colony forming units (CFUs) CFU-GEMM, CFU-GM, CFU-G, CFU-M, and CFU-E, and the burst forming unit BFU-E colonies, by testing two different CD-160130 concentrations (5 and 10 μM). CD-160130 was preincubated with 2×10^4 BM cells/35 mm dishes for 15 minutes. Cells were then maintained in a humidified atmosphere and 5% CO_2. Colonies were enumerated using an inverted microscope after 18 days of culture according to the manufacturer's protocol. The results were the average of three independent experiments from three different patients.

Cell Viability, Cytotoxicity, and Proliferation. To assess cell viability the WST-1 cell viability assay (Roche Diagnostics, Mennheim, Germany) was used. Leukemia cells were serum starved for 16 hours with 1% fetal bovine serum and were subsequently seeded at 3×10^4/well in 96-well plates, and incubated with CD-160130 for 24 hours. PBMNCs were seeded (6×10^4/well) in 96-well plates, and incubated with CD-160130 for 6 hours without stimulation. In both cases at the end of incubation the WST-1 reagent was added and absorbance was measured at 450 nm. The mean and S.D. were calculated for each group and average data fitted using a Hill-type equation (see Supplemental Material). The ED_{50} value was calculated from the dose-response curve interpolating the experimental data (Microcal Origin 8.0 software; OriginLab Corporation, Nothampton, MA). For the cytotoxicity assay CLL cells (2.5×10^5/well) were seeded in 96-well plates and incubated with CD-160130 (0.1–100 μM) for 72 hours. Cytotoxicity was detected using the CellTiter 96 Aqueous One Solution Cell Proliferation Assay kit (Promega, Madison, WI). Optical densities were measured at 490 nm. The EC_{50} value was determined from a two-point linear regression of the two concentrations of CD-160130 that induced greater than and less than 50% CLL cell death. The EC_{50} was the concentration on the linear regression curve that corresponded to 50% viability. To assess cell proliferation 1×10^4 cells/well were seeded in 96-well plates and treated with CD-160130 at time 0 (single treatment) or at both time 0 and 48 (double treatment). Following incubation, cells were harvested and counted using a Bürker chamber with viable cells identified as trypan blue negative.

Electrophysiological Experiments

Patch-Clamp Recording. Membrane currents were recorded in the whole-cell configuration of the patch-clamp technique at room temperature (about 25°C) by using a Multiclamp 700A amplifier (Molecular Devices, Sunnyvale, CA). Micropipettes (3–5 MV) were pulled from borosilicate glass capillaries (Harvard Apparatus, Holliston,

MA), with a PC-10 pipette puller (Narishige, Tokyo). Series resistance was always compensated (up to approximately 80%). Currents were low-pass filtered at 2 kHz and digitized online at 10 kHz, with Digidata 1322A and pClamp 8.2 (Molecular Devices, Sunnyvale, CA). Data were analyzed off-line with pClamp and Origin 8.0 (Microcal, Inc., Northampton, MA) software. To measure $K_V11.1$, $K_{ir}2.1$, and $K_V1.5$ currents, the pipette solution contained (in mM): K^1 aspartate 130, NaCl 10, $MgCl_2$ 2, $CaCl_2$ 2, HEPES 10, and EGTA 10, titrated to pH 7.3 with KOH. During the experiments, cells were perfused with an extracellular solution containing (in mM): NaCl 130, KCl 5, $CaCl_2$ 2, $MgCl_2$ 2, HEPES 10, and Glucose 5, adjusted to pH 7.4 with NaOH. In this case, the K^1 equilibrium potential (E_K) was 280 mV. When necessary, a high extracellular [K^1] (40 mM) was applied to increase the amplitude of inward $K_V11.1$ currents measured at 2120 mV, thus avoiding the necessity of applying excessively negative potentials. In this case, the NaCl and KCl concentrations were 95 and 40 mM, respectively (E_K 5 230 mV). To measure the $K_{Ca}3.1$ and $K_V1.3$ currents, the pipette and extracellular solutions were prepared as in Sankaranarayanan et al. (2009) and Zimin et al. (2010), respectively. The current-voltage relationship for $K_V11.1$ was determined from peak tail currents at 2120 mV (for 1.1 second), following 15 second conditioning potentials from 0 to 270 mV (10 mV steps). The time between consecutive trials in the same stimulating protocol was 4 seconds. The holding potential (V_H) was 0 mV. The same stimulation protocol was used to determine the concentration-response relationships for CD-160130, CD-140793, and E4031. For clarity, in Fig. 2, B–D, we only reported the drug effect on the tail currents elicited after conditioning at 0 mV. The current-voltage relationships were determined for $K_{ir}2.1$ from measurements of peak current amplitude at 2110 mV (for 500 milliseconds). For $K_V1.3$ and $K_V1.5$ the current-voltage relationships were determined from measurements of peak current amplitude at 140 mV (for 500 milliseconds), starting from a V_H value of 280 or 260 mV, respectively. The $K_{Ca}3.1$ currents were elicited by voltage ramp protocols as in (Sankaranarayanan et al., 2009) and the decrease of slope conductance was taken as a measure of channel block. Each compound was applied for at least 4 minutes (or until steady-state inhibition was attained), with each concentration being tested on at least five different cells. At the end of each application, drugs were washed out for at least 2 minutes. As positive controls, we used E4031 (for $K_V11.1$), 100 *m*M $BaCl_2$ (for $K_{ir}2.1$), 50 *m*M nifedipine (for $K_V1.5$), 10 nM margatoxin (for $K_V1.3$), and 25 nM TRAM-34 (for $K_{Ca}3.1$). Dimethylsulfoxide (DMSO), which served as the solvent for CD-160130 and CD-140793, was used as the negative control.

Perforated Patch Recordings of Cardiac Myocyte APs. Bo- rosilicate standard wall without filament glass electrodes (Harvard Apparatus) were pulled to a resistance of 1.5–2.5 MV. Electrodes were tip-filled (2–3 mm) with amphotericin-B-free solution and back-filled with intracellular pipette solution containing 0.48 mg/ml amphotericin-B (Apollo Scientific, Stockport, United Kingdom). Current-clamp recordings were made using an Axopatch 200B amplifier, Axon 1322A digidata, and Clampex 8.2 (Molecular Devices, Sunnyvale, CA). APs were stimulated at 2 Hz in modified extracellular solution (4 mM KCl, 1 mM $MgCl_2$) and at 37°C. APs were sampled at 10 kHz and on-line filtered at 5 kHz. 20 APs were signal averaged after stabilizing in the control or CD-160130-containing Tyrode.

Analysis of Electrophysiological Experiments. The concentration-response relationships for the different drugs were obtained by plotting the percentage residual currents versus the drug concentration. The residual currents were calculated through the following

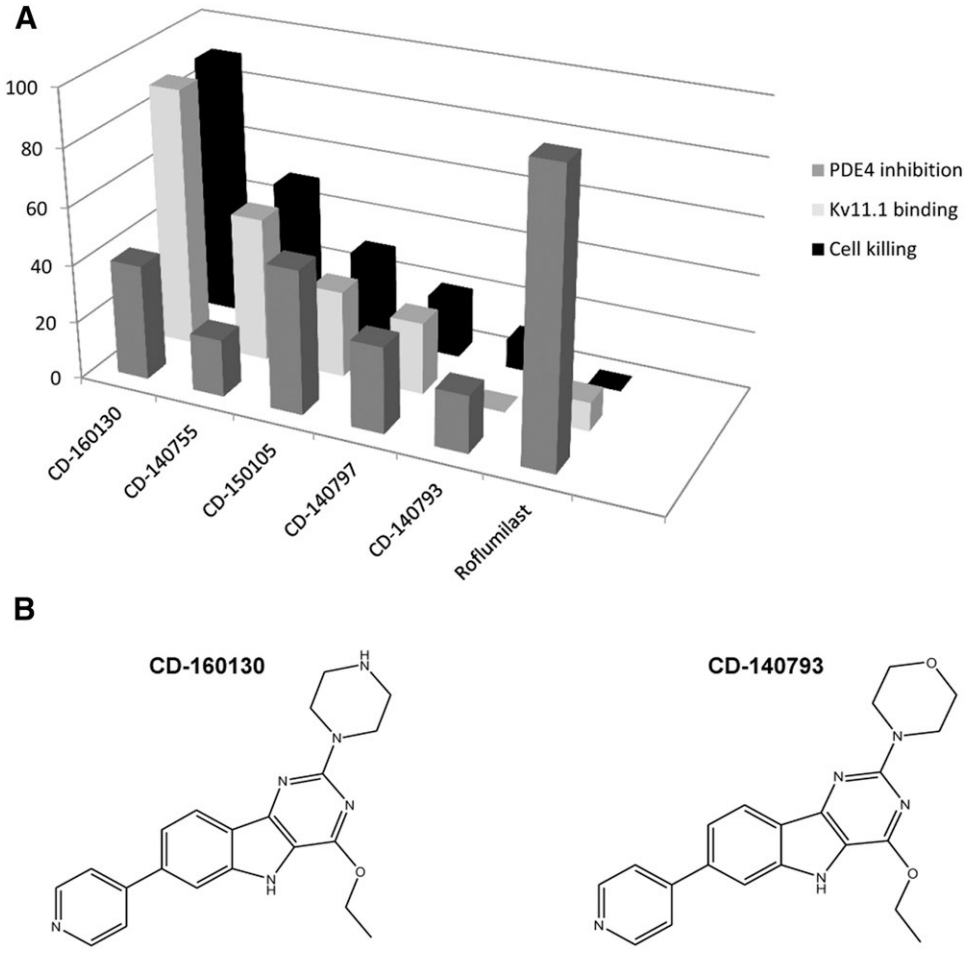

Fig. 1. Disparity between CLL killing activities and PDE-4 inhibition. (A) Three-dimensional graph showing the comparison between CLL killing, PDE-4 inhibition, and $K_V11.1$ binding for CD-160130, some analogs and roflumilast (a selective PDE-4 inhibitor). Each data series is reported as a percentage normalized to the highest values. Original values of EC_{50}, IC_{50}, and B_{50} for each analog are reported in Supplementary Table 1. CLL cell killing was performed on primary CLL samples obtained from peripheral blood of patients enrolled at the University of Leipzig and evaluated with CellTiter 96 Aqueous One Solution Cell Proliferation Assay kit; PDE-4 inhibition was analyzed with SPA assay and $K_V11.1$ binding was performed with [^{3}H] astemizole binding assay (see Supplemental Material). (B) Chemical structure of CD-160130 and of the structural analog CD-140793.

formula: $100 \times I_{max\ drug}/I_{max\ contr}$, where $I_{max\ drug}$ is the maximal current in the presence of a given drug concentration and $I_{max\ contr}$ is the maximal current in the absence of the drug; for $K_V11.1$ the maximal tail current is the current at peak subtracted from the holding current. The mean and S.E.M. were then calculated for each drug concentration and the average data points fitted using a Hill-type equation, $y = A_0 + (A_1 - A_0) \times [x^n/(k^n + x^n)]$, where A_0 is the minimum and A_1 is the maximum of the function; x is the drug concentration; k is the IC_{50} value; and n is the Hill coefficient. The IC_{50} value was calculated from the concentration-response curve interpolating the experimental data using the Microcal Origin software; OriginLab Corporation.

In Vivo Experiments

The in vivo experiments on mice and guinea pigs are ex- tensively described in the Supplemental Material. All experi- ments on live vertebrates have been carried out in accordance with the Principles of Laboratory Animal Care (directive 86/609/ EEC).

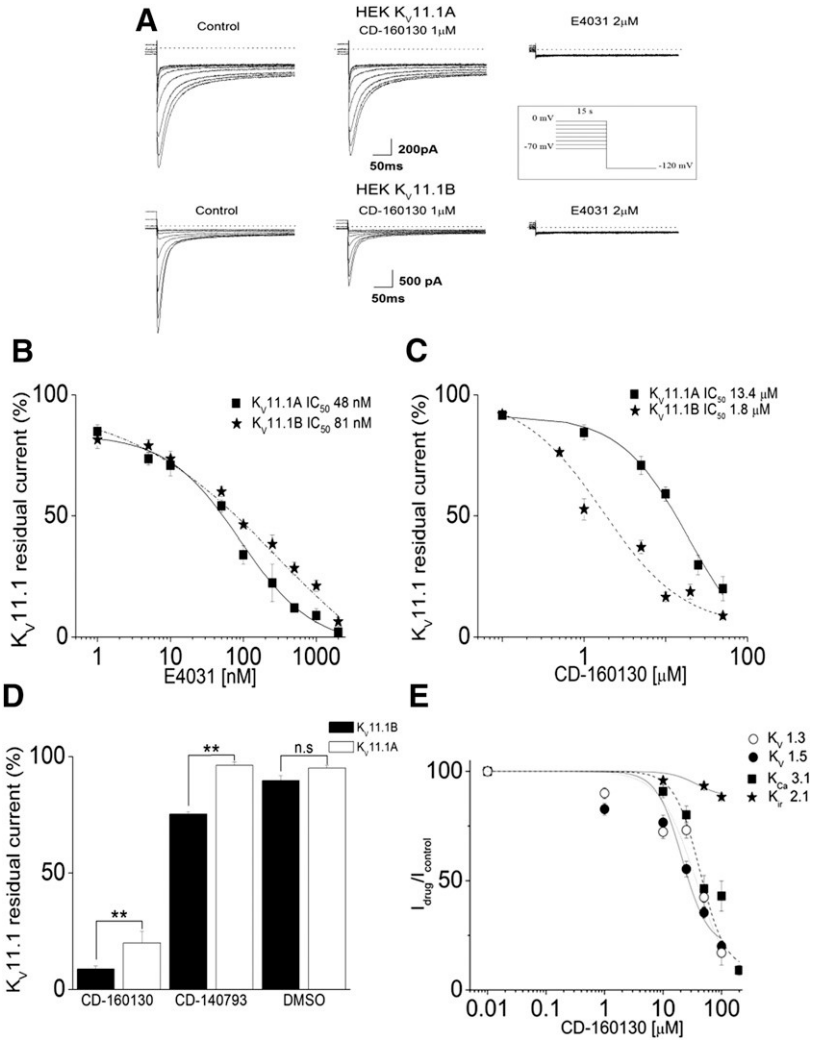

Fig. 2. CD-160130 and E4031: $K_V11.1$ blockers with different isoform selectivity. (A) Typical $K_V11.1A$ and $K_V11.1B$ currents in stably transfected HEK 293 cells and the effect of the selective $K_V11.1$ inhibitor E4031 and CD-160130. The inset shows the protocol used to record the tail current. The main functional difference between the two isoforms consists of the more rapid deactivation kinetics of $K_V11.1B$, which is apparent when comparing the upper ($K_V11.1A$) and the lower ($K_V11.1B$) panels in Fig. 1A. Both currents were fully blocked by 2 *m*M E4031, a class III antiarrhythmic drug considered the prototype of $K_V11.1$ blockers. (B) Concentration-response curves and IC_{50} values obtained with E-4031 on transfected HEK 293 cells. At both 50 and 100 nM, no significant difference was observed between the effects produced on $K_V11.1A$ or $K_V11.1B$ ($P = 0.407$ and 0.426, respectively; $n = 6$). (C) Concentration-response curves and IC_{50} obtained with CD-160130 on transfected HEK 293 cells. Full concentration-response relationships were obtained for both E4031 and CD-160130 by measuring the percentage residual tail currents at different drug concentrations, after a 15 second pulse at 0 mV. The applied protocol is shown in the inset in (A) and detailed in Materials and Methods. (D) Bars give $K_V11.1$ residual current in the presence of CD-160130 (50 *m*M), CD-140793 (50 *m*M), and DMSO. A significant difference was found between inhibition of $K_V11.1A$ and $K_V11.1B$ with both compounds ($P < 0.01$ for CD-160130 and $P < 0.01$ for CD-140793; $n = 6$), although the degree of inhibition was higher in the CD-160130 group. DMSO, used for the solubilization of CD-160130 and CD-140793, produced no effect on either $K_V11.1$ isoform at the maximum concentration used (1% v/v). (E) Concentration-response relationships obtained with CD-160130 on cells transfected with $K_{ir}2.1$ (solid stars), $K_V1.3$ (open circles), $K_V1.5$ (solid circles), or $K_{Ca}3.1$ (solid squares). For $K_{ir}2.1$ we measured the percentage residual steady-state currents at different drug concentrations at 2110 mV (V_H was 270 mV). For $K_V1.3$ we measured the percentage residual currents at different drug concentrations at +40 mV (from a V_H of 280 mV) following the procedures as in Zimin et al. (2010). For $K_V1.5$ we measured the percentage residual currents at different drug concentrations at +40 mV (from a V_H of 260 mV). $K_{Ca}3.1$ currents were elicited by voltage ramps from 2120 to +50 mV (from a V_H of 280 mV). The fold decrease of slope conductance was taken as a measure of channel block. For $K_V1.5$, $K_{Ca}3.1$, and $K_{ir}2.1$ HEK transfected cells were analyzed; for $K_V1.3$, L929 cells were used.

Chemicals and Drugs

CD-160130 and related analogs were synthesized as in Reichelt et al. (2014). Stock solutions (5 and 10 mM) of CD-160130 and CD-140793 (BlackSwanPharma GmbH, Leipzig, Germany) were prepared in DMSO for in vitro experiments. The maximal DMSO concentration for in vitro experiments was 1% v/v. In particular, for patch-clamp experiments the effects of DMSO on the currents were subtracted from the effects of CD-160130 at the highest tested concentration. For ECG measurement, CD-160130 (10 mg/kg) was suspended in 5% Kolliphor in 0.9% NaCl. Ora-Plus (Paddock Laboratories, Inc., Minneapolis, MN) was used as the vehicle for oral gavage administration of CD-160130 in mice experiments.

Amphotericin B (60 mg/ml) was dissolved in DMSO. E4031 (Alomone Laboratories, Jerusalem, Israel) was dissolved in water (stock solution of 5 mM). Stock solution of cytarabine, doxorubicin (Amersham, GE Healthcare Pittsburgh, PA; 50 mg doxorubicin chlorohydrate in NaCl, pH of 3) and fludarabine used in the co-culture experiments were prepared in distilled water. Sotalol, used for the ECG measurement was dissolved in 0.9% NaCl. Unless otherwise indicated, chemicals were purchased from Sigma Chemicals (St Louis, MO).

Statistical Analysis

All averaged data are presented as mean 6 S.E.M. (or S.D. when specified).The statistical significance of differences between experimental groups was calculated with the Mann-Whitney test, with a P , 0.05 being considered as statistically significant. When specified (see the legends to Fig. 5D and Fig. 7, B and C), the Student's t test was applied.

Information concerning guinea pig cardiac myocyte isolation, astemizole binding assay, PDE-4 inhibition assay, apoptosis analysis, bromodeoxyuridine assay, RNA interference, real-time quantitative polymerase chain reaction, Western blot, vectors, and in vivo experiments (pharmacodynamics, pharmacokinetics, and ECG recordings) are detailed in the Supplemental Material. Written informed consent was obtained from all patients (mixed sex) or their legal guardians prior to sample collection, according to the Declaration of Helsinki.

Results

Pharmacological Properties of CD-160130. The pyrimidoindole CD-160130 was originally developed as a PDE-4 inhibitor with the aim of developing a drug able to promote apoptosis in leukemic cells through an increase in intracellular cAMP levels (Kim and Lerner, 1998; Lerner and Epstein, 2006). Indeed, CD-160130 was shown to possess a cytotoxic effect on primary CLL cells (Weinberg et al., 2007). However, discrepancies between the PDE-4 inhibitory activity and cytotoxic efficacy for CD-160130 and some of its close analogs emerged (see Supplemental Table 1), suggesting that the inhibition of PDE-4 is unlikely to play a major role in these effects. Supplemental Table 1 also shows that several of these compounds also bind $K_V11.1$ channels expressed in HEK 293 cells, as measured by the astemizole binding assay. As is evident from Fig. 1, $K_V11.1$ binding efficacy better correlated with CLL cell killing than PDE-4 inhibition. In particular, CD-160130 had the highest $K_V11.1$ binding affinity (B_{50} 5 1.89 mM; Supplemental Table 1) and the highest current blocking effect. This was correlated with a high cytotoxic capacity and yet low PDE-4 inhibition. In contrast, CD-140793 (a structural analog of CD-160130, which differs by a single substitution in the R4 position of the molecule) did not bind $K_V11.1$ and did not show any antileukemic effect, despite displaying similar inhibitory activity on PDE-4 (Supplemental Table 1). These data prompted us to evaluate whether the effect of CD-160130 on leukemic cells was caused by a blocking effect on $K_V11.1$ currents.

CD-160130 Blocks $K_V11.1$ Currents. Leukemia cells express the A and B isoforms of $K_V11.1$, but tend to overexpress $K_V11.1B$ (Crociani et al., 2003; Pillozzi et al., 2007, 2011, 2014). Hence, we tested the effect of CD-160130 on either isoforms, expressed in HEK 293 cells (Fig. 2). Currents were measured as tail currents at 2120 mV, after depolarizing voltage steps ranging from 0 to 270 mV and lasting 15 seconds (Fig. 2A, inset). The classic $K_V11.1$ blocker E4031 produced similar effects on both channel isoforms (Fig. 2B). On the other hand, CD-160130 had a 7.6-fold higher selectivity for $K_V11.1B$ (IC_{50} 5 1.8 6 0.26 mM; Hill coefficient 5 0.88 6 0.25) than for $K_V11.1A$ (IC_{50} 5 13.4 6 3.0 mM; Hill coefficient 5 1.1 6 0.1) (Fig. 2C). The difference between the IC_{50} values was statistically significant (at 1 mM, P , 0.01; n 5 6). As shown by the data on N-deleted mutants (Supplemental Fig. 1), the different efficacies of CD-160130 and E4031 on the two $K_V11.1$ isoforms did not depend on the peculiar $K_V11.1B$ N-terminal domain (Supplemental Fig. 1).

As expected, CD-140793 produced negligible (on $K_V11.1A$) or small (on $K_V11.1B$) current inhibition, even at very high concentrations (50 mM; Fig. 2D). Nonetheless, both CD-160130 and CD-140793 produced significantly stronger inhibition of $K_V11.1B$ (P , 0.01; at 50 mM; n 5 6).

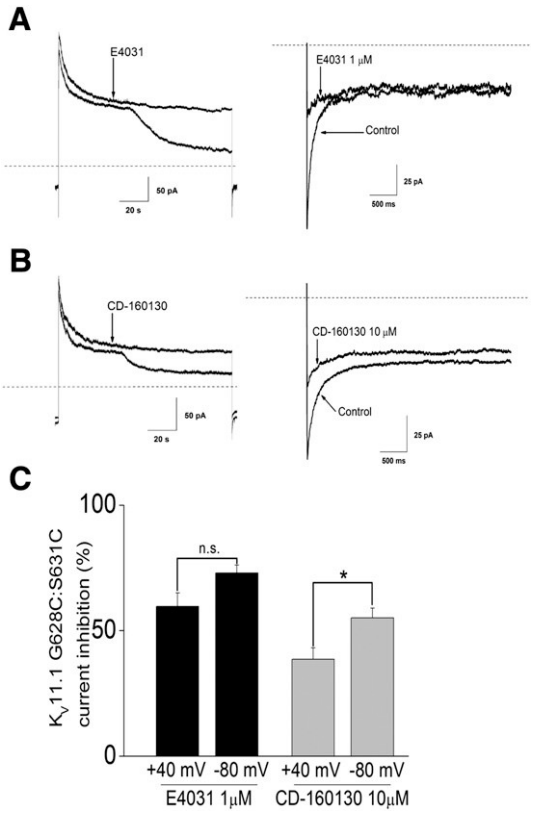

Fig. 3. CD-160130 demonstrates blocking features different from E4031. (A and B) currents elicited in the G628C:S631C $K_V11.1$ mutant and effects of 1 mM E4031 and 10 mM CD-160130. (C) $K_V11.1$ current inhibition by E4031 and CD-160130 at the two tested potentials (+40 and 280 mV); for E4031 the difference between the inhibition at +40 and 280 mV was not statistically significant (P . 0.05; n = 5), while a significant difference was obtained for CD-160130 (P , 0.05; n = 9).

We also evaluated the effects of CD-160130 on other K^1 channels known to be expressed in lymphoid or myeloid cells, such as $K_{ir}2.1$, K_V 1.3, $K_V1.5$, and $K_{Ca}3.1$. These were expressed in HEK 293 cells (Fig. 2E). CD-160130 produced only 12% inhibition of $K_{ir}2.1$ currents at 100 *m*M, while it inhibited K_V 1.3, $K_V1.5$, and $K_{Ca}3.1$ in a dose-dependent manner (the IC_{50} values were 36.7 6 5.7, 26.05 6 6.25, and 53.5 6 7.05 *m*M, respectively).

Kinetics and Voltage Dependence of Channel Inhibition. At the maximum concentrations of CD-160130 tested, the current inhibition was reversed after 258 6 20 seconds of washing (n 5 5). This is different from what we normally observe with E4031, whose block is notoriously difficult to reverse by washout (Faravelli et al., 1996), and suggests that the blocking mechanism of CD-160130 is different from that of E4031. This was further investigated by testing the CD-160130 effect on the non-inactivating G628C: S631C $K_V11.1$ mutant. The absence of channel inactivation enabled us to (1) study the kinetics of channel block and (2) compare the effects of outward and inward ion fluxes on the CD-160130 potency. In these measurements, E_K was set to 230 mV, to make it practical to compare inhibition of both outward and inward currents. Currents were elicited, from a V_H of 280 mV, by a 120 second step to 140 mV. Next, V_m was stepped back to 280 mV, to reveal the inward tail currents. Either CD-160130 (10 *m*M) or E4031 (1 *m*M) was applied after the current had reached steady state at 140 mV. Typical current traces are shown in Fig. 3A. For clarity, the tail currents at 280 mV are magnified in Fig. 3B. In a series of representative experiments carried out in the same batch of cells, CD-160130 took about 7.4 6 1.25 (n 5 6) s to start

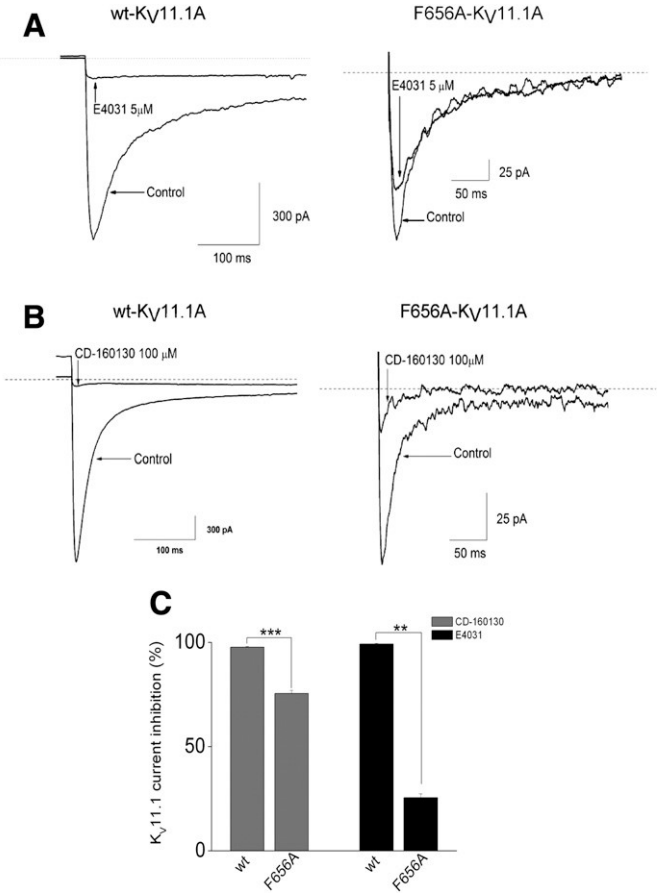

Fig. 4. Effect of CD-160130 on the F656A-$K_V11.1A$ mutant. (A) Effect of E4031 (5 *m*M) on wild-type $K_V11.1A$ and F656A- $K_V11.1A$ channels transiently expressed in Chinese hamster ovary cells. (B) Effect of CD-160130 (100 *m*M) on wild-type $K_V11.1A$ and F656A-$K_V11.1A$ channels transiently expressed in Chinese hamster ovary cells. (C) Bars give the percentage of $K_V11.1$ current inhibition with CD-160130 and E4031. *** = P , 0.001; **= P , 0.01. A significant difference was also found between the effects of E4031 and CD-160130 on $K_V11.1$-F656A current (P , 0.01; n = 5 for E4031; n = 10 for CD-160130).

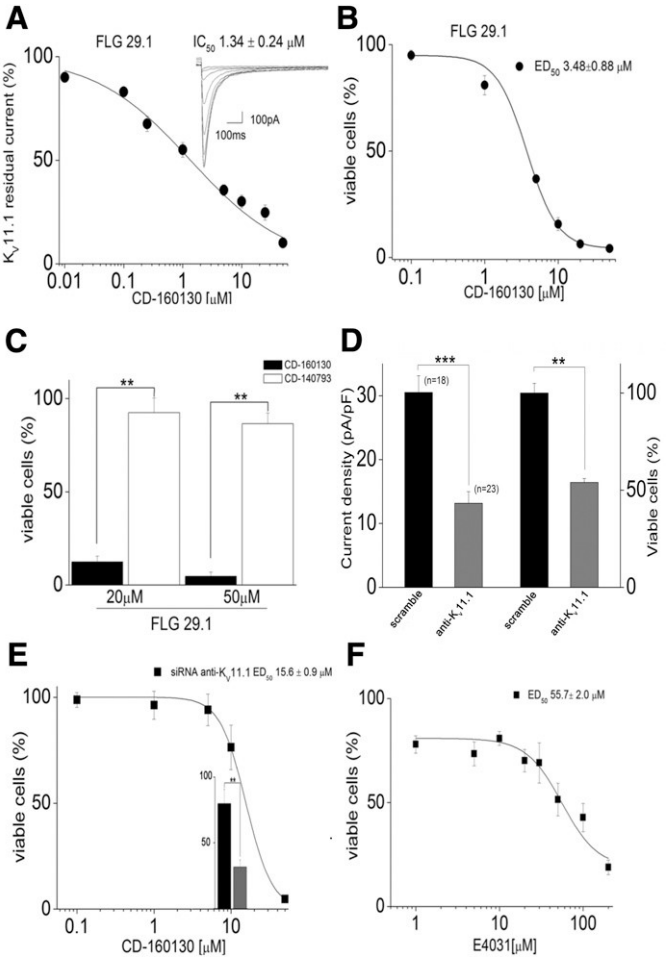

Fig. 5. CD-160130 displays antileukemic capacity in vitro. (A) Concentration-response curves and IC_{50} values obtained with CD-160130 on FLG 29.1; the inset shows a typical $K_V11.1B$ current in FLG 29.1 cells. (B) Concentration-response curves and ED_{50} values obtained with the WST-1 cell viability assay on FLG 29.1. Experimental data were normalized to control untreated cells and fitted with a Hill-type equation (see *Materials and Methods*). (C) Bars give the results obtained with the WST-1 cell viability assay of CD-160130 and CD-140793 on FLG 29.1 cells. A significant difference was found between the effects of CD-160130 and CD-140793 (P , 0.01 at 20 and 50 *m*M, repectively; n = 9). (D) Bars on the left show the Kv11.1 current density of FLG 29.1 cells 48 hours after transfection with scrambled siRNAs (black bars) or anti-Kv 11.1 siRNAs (gray bars). Bars on the right show the number of viable cells in the same conditions, obtained with the WST-1 cell viability assay. In these experiments, the WST-1 assay was carried out in triplicate on the cells taken directly from the cultures treated with either scrambled or anti-$K_V11.1$ siRNAs **P = 0.01 (Student's t test); ***P , 0.001 (Mann-Whitney test). (E) Concentration-response curves and ED_{50} values obtained with CD-160130 on siRNA anti- $K_V11.1$ transfected FLG 29.1 cells; in the inset is shown a comparison of cell viability between scrambled siRNA (gray) and anti-$K_V11.1$ siRNA (black) transfected cells at 10 *m*M CD-160130. (F) Concentration-response curves and ED_{50} values obtained with E4031 on FLG 29.1.

blocking $K_V11.1$ current at 140 mV. In contrast, the effect of E4031 had a latency of 18 6 1.4 seconds (n 5 5; P , 0.01 compared with the CD-160130 values). We next compared the effect of the two blockers on outward (at 140 mV) and inward (at 280 mV) currents (Fig. 3C). For E4031, inverting the current flow by reversing the V_m polarity produced no significant difference in channel block (P . 0.05; n 5 5), whereas CD-160130 had a slightly more pronounced effect on inward currents (55.16 3.9, n 5 7, P , 0.05). Finally, the effect of CD-160130 showed negligible voltage dependence (see Supplemental Fig. 2).

Effect of CD-160130 on the F656A-$K_V11.1A$ Mutant. E4031 and similar drugs block $K_V11.1A$ and $K_V11.1B$ isoforms by binding to aromatic residues in the channel inner cavity, particularly Phe656 (Kamiya et al., 2006). To study whether CD-160130 acts with a similar mechanism, we compared the inhibition produced by saturating concentrations of either E4031 (5 *m*M) or CD-160130 (100 *m*M) on $K_V11.1A$ and F656A-$K_V11.1A$ channels. As expected, E4031 almost abolished the $K_V11.1A$ currents, while producing approximately only 25% inhibition of the F656A-$K_V11.1A$ current (Fig. 4, A and C). In contrast, CD-160130 produced about 98% inhibition of $K_V11.1A$ and 75.5% inhibition of F656A-$K_V11.1A$ (Fig. 4, B and C). Detailed statistics are given in the legend to Fig. 4. These results suggest that Phe656 is not part of the main binding site for CD-160130.

Effect of CD-160130 on Leukemia Cell Vitality and Proliferation. To verify whether CD-160130 also blocked $K_V11.1$ in leukemia cells we used FLG 29.1, an AML cell line that mainly expresses the $K_V11.1B$ isoform (Crociani et al., 2003, see the inset to Fig. 5A). As shown in Fig. 5A, the IC_{50} obtained for CD-160130 on FLG 29.1 cells (1.34 6 0.24 *m*M) was very similar to that obtained on HEK 293 cells transfected with $K_V11.1B$, supporting the notion that CD-160130 exhibits isoform selectivity.

Next, we investigated the effects of CD-160130 (0.1–50 *m*M) on FLG 29.1 cell viability, evaluated by either WST-1, trypan

TABLE 1

Effect of CD-160130 on viability of leukemia primary samples and cell lines.

Mean ED_{50} values and S.E.M. obtained with CD-160130 on both myeloid and lymphoid primary samples as well as in a panel of leukemic cell lines (AML and ALL). For each primary sample and cell line the French-American-British classification, the immunophenotype, and the cytogenetics (if available) are also reported, along with *KCNH2b* and *KCNH2a* genes expression. *KCNH2* isoforms expression was evaluated through real-time quantitative polymerase chain reaction and is reported as arbitrary units normalized on different calibrators in accordance with their cellular origin: in particular, the myeloid primary samples were obtained from peripheral blood and calibrated on PBMNCs, the lymphoid primary samples were obtained from BM and calibrated on $CD19^+$ cells (B-ALL-1) or $CD3^+$ cells (T-ALL-1). All the data were the average 6 S.E.M.

PS/Cell Line	FAB (Immunophenotype)	Cytogenetics	*1B* Gene Expression	Mean ED_{50} (6 S.E.M.) of CD-160130
			Arbitrary Units	*m*M
Myeloid primary samples and cell lines				
AML-1 (Pillozzi et al., 2007)	AML-M4 (CD13+, CD33+, CD14+, CD11b+, CD34+)	UNK	0.92 (1A: 12.20)	20% maximum killing at 50
AML-2 (Pillozzi et al., 2007)	AML-M1 (CD13+, CD34+, HLDRA+)	Complex	68.10 (1A: 18)	40.4 6 11.2
KG-1	AML-M6 (CD34+, CD15+, Cd13+, HLA A30+, A31+, B35+)	Complex (Pelliccia et al., 2012)	0.62 (1A: 24.76)	7.6 6 0.55
FLG 29.1	AML-M5 (CD9+, CD13+, CD32+, CD42b+, CD51+, CD54+, CD44+, CD61+, CD45+, CD31+)	polyploidy, 3p+	3413 (1A: 1086)	3.48 6 0.88
HL60	AML-M2 (Dalton et al., 1988) (CD32, CD13+, CD142, CD15+, CD192, CD33+, HLA-DR2)	Pseudodiploid	94.70 (1A: 13.70)	6.65 6 0.26
NB4	AML-M3 (CD32, CD4+, CD11b2, CD13+, CD14-, CD15+, CD19-, CD33+, CD342, CD38+, HLA-DR2)	t(15;17)(q22;q11-12)	196.72 (1A: 80.44)	7.02 6 0.31
Lymphoid primary samples and cell lines				
B-ALL-1	L2 (early B) (CD34+, CD33+, CALLA+)	t(8;14)	6.68 (1A: 0.03)[a]	5.6 6 1.5
T-ALL-1	L2 (T) (aberrant expression of CD34, CD117, and CD13)	UNK	5.11 (1A: 0.76)[b]	0.6 6 0.2
REH	pro-B-ALL (CD32, CD10+, CD132, CD19+, CD342, CD372, CD38+, cyCD79a+, CD802, CD138+, HLA-DR+, sm/cyIgG2, sm/cyIgM2, sm/cykappa2, sm/cylambda2)	t(12; 21)(p13;q22)	120 (1A: 6.5)	6.66 6 0.22
697	pre-B-ALL (CD32, CD10+, CD132, CD19+, CD342, CD372, CD38+, CD802, HLA-DR+, sm/cyIgG2, smIgM2, cyIgM+, sm/cykappa2, sm/cylambda2)	t(1;19)	1200 (1A:85)	3.78 6 0.37
RS	pre-B-ALL-L2 (HLA DR+, CD9+, CD24+)	t(4;11)(q21; q23) and i(7q)	0.16 (1A: 0.005)	7.0 6 0.2

B-ALL, acute B-lymphoid leukemia primary sample; FAB, French-American-British; PS, primary sample; T-ALL, acute T-lymphoid leukemia primary sample; UNK, unknown; 1A, *KCNH2a*; 1B, *KCNH2b*.

[a] *1A* and *1B* values were average expression of a cohort of BCP-ALL patients.

[b] *1A* and *1B* values were average expression of a cohort of T-ALL patients.

TABLE 2

Effect of CD-160130 on viability of normal and solid tumor cell lines.

Data gathered with CD-160130 on two normal cell lines (PBMNC and EBV-infected B-lymphocytes) and on a tumour cell line (HCT116) are reported, together with the KCNH2b gene expression. A direct comparison between the expression of the two transcripts (KCNH2a and KCNH2b) was not feasible, because of the different sensitivity of the primers used to detect the two transcripts. All the data were the average 6 S.E.M.

PS / Cell line	*1B* gene expression (arbitrary units)	Mean ED_{50} (6SEM) of CD-160130
PBMNC	0 (1A: 0)	37% maximum killing at 10 mM
EBV-infected B lymphocytes	0 (1A: 0)	17% maximum killing at 10 mM
HCT116	0 (1A: 62.4) (Crociani et al., 2013)	11.94 6 0.92 mM

EBV, Epstein-Barr Virus; 1A, *KCNH2a*.

blue, or bromodeoxyuridine assay. Since the three assays gave virtually identical results (Supplemental Table 2), we will only show the data obtained with the WST-1 assay (Fig. 5B; Tables 1, 2 and 3). FLG 29.1 cell viability was markedly reduced by CD-160130 at micromolar concentrations (Fig. 5B). The effective dose (ED_{50}) turned out to be 3.48 *m*M (Fig. 5B; Tables 1–3). Conversely, CD-140793, which does not block K_V11.1 currents, produced little effect on FLG 29.1 even at high concentrations (50 *m*M; Fig. 5C). To test whether the effect of CD-160130 on FLG 29.1 was related to the blocking of K_V11.1, we silenced *KCNH2* with small interfering RNAs (siRNAs). Since FLG 29.1 cells almost exclusively express K_V11.1B (Crociani et al., 2003), the siRNAs we used, which target a *KCNH2* sequence common to both *KCNH2a* and *KCNH2b*, and indeed silenced KCNH2b in these cells. Compared with scrambled siRNAs, anti-K_V11.1 siRNAs reduced the K_V11.1 current density of FLG 29.1 and the number of viable cells by roughly the same extent (55%) 48 hours after transfection (Fig. 5D). Moreover, the ED_{50} of CD-160130 on anti-K_V11.1 siRNA-treated cells was 15.6 *m*M (Fig. 5E). A significant difference in the percentage of viable cells was detected at 10 *m*M (P , 0.01, n 5 9; inset to Fig. 5E). As expected, scrambled siRNA had virtually no effects on CD-160130 ED_{50} (Supplemental Fig. 3). These results are consistent with CD-160130 reducing the viability of FLG 29.1 cells through a K_V11.1B-dependent mechanism. The isoform-nonselective K_V11.1 blocker E4031 reduced FLG 29.1 cell viability, although with a significantly higher ED_{50} (55.7 *m*M; Fig. 5F). It is worth noting that E4031 was efficacious at concentrations comparatively high relative to those required to block the channel (Fig. 2B). This is normally observed when using this drug and is caused by a lower free concentration in complex, protein-rich, media (Masi et al., 2005).

The effect of CD-160130 on the viability of further leukemia cell lines and primary samples (either AML or ALL) is shown in Table 1. CD-160130 turned out to be cytotoxic toward different leukemia cells in the micromolar range. CD-160130 did not affect cell viability of either normal PBMNC or Epstein-Barr virus–infected B lymphocytes (Tables 2).

We also evaluated whether CD-160130 displayed BM toxicity by testing the compound on the clonogenic potential of BM cells from three healthy donors. CD-160130 did not affect either the number of CFUs, or the percentage of different CFUs at 5 *m*M concentration, but only produced a weak, not statistically significant, reduction in the overall number of colonies at 10 *m*M (Tables 3).

Collectively, the cytotoxic effect of CD-160130 was more evident when more *KCNH2b* transcript (measured by real-time quantitative polymerase chain reaction) was expressed by leukemic cells. Consistently, a good relationship emerged between the efficacy of CD-160130 and the amount of K_V11.1B protein (Supplemental Fig. 4). In contrast, the K_V11.1A-expressing HCT116 colorectal cancer cells (Crociani et al., 2013) were less sensitive to CD-160130 (ED_{50} 11.9 *m*M, Table 2).

We also studied the effects of CD-160130 on CLL primary samples, similar to those analyzed in Fig. 1, to determine whether the effect was related to a specific mutation status (Table 4). CLL cells express K_V11.1 (Smith et al., 2002), and the expression of the *KCNH2b* transcript (Supplemental Table 3) and of the K_V11.1 current (Supplemental Fig. 5) was confirmed in the MEC1 cell line. As previously reported (Weinberg et al., 2007), CLL cells were sensitive to the drug. CD-160130 was more efficacious on CLL samples deleted both in 13q and 11q, which responded poorly to fludarabine (Table 4).

Finally, we evaluated whether CD-160130 inhibited leukemia cell proliferation. After a single treatment, leukemia cell proliferation was completely abolished at concentrations above 5 *m*M (Fig. 6A). The effect was more evident on 697 and REH, where concentrations between 1 and 5 *m*M were also efficacious. At lower concentrations, after an initial block (lasting about 24 hours), FLG 29.1 and HL60 cells started to proliferate again. The effect was potentiated by subsequent readministration. For example, when CD-160130 was readded to the cells after 48 hours, the inhibition of cell proliferation was sustained (in FLG 29.1, Fig. 6B) or complete (in HL60, Fig. 6B). Under these conditions, even 0.1 *m*M produced a significant reduction of cell proliferation. This is consistent with the pharmacokinetics of CD-160130 in vivo and the antileukemic effects in vivo, as will be discussed below.

Effect of CD-160130 on Leukemia Cell Apoptosis and Related Signaling. Next, we studied whether the cytotoxic effect of CD-160130 on leukemia cells was, at least in part, related to apoptosis. This point was determined on leukemic

TABLE 3

Evaluation of CD-160130 toxicity in healthy human bone marrow colonies.

Results of the overall colony numbers obtained with clonogenic assay of three samples of healthy bone marrow treated with two different concentrations of CD-160130 (5 and 10 mM) are reported. The different colony fractions (CFU-GEMM, CFU-GM, CFU-G, CFU-M, CFU-E and BFU-E) for each group are reported. All the data were average 6 S.E.M.

	Total CFU Number	CFU-GEMM Fraction	CFU-GM Fraction	CFU-G Fraction	CFU-M Fraction	BFU-E Fraction	CFU-E Fraction
	%	%	%	%	%	%	%
Control	100	5 6 1	19.5 6 2.5	15 6 3	31 6 3	7 6 1	22.5 6 1.5
CD-160130 (5 *m*M)	97 6 5.2	5.5 6 1.5	21.5 6 2.5	14 6 3	28.5 6 2.5	6.5 6 0.5	24 6 2
CD-160130 (10 *m*M)	75 6 8.8	4 6 1	18 6 1	13 6 3	25 6 1	9 6 0	31 6 1

BFU, burst forming unit.

TABLE 4

-CLL primary samples and cell line cytotoxic effect of CD-160130

Mean EC_{50} values and S.D. obtained with CD-160130 on primary B-CLL samples (isolated from peripheral blood of patients enrolled at the University of Leipzig) and on the MEC1 cell line. For each sample, the Binet stage and cytogenetics (if available) are also reported.

Primary Sample/Cell Line	Binet Stage	Gender	Cytogenetics	Mean EC_{50} (6 S.D.) of CD-160130	Mean EC_{50} (6 S.D.) of Fludarabine
				*m*M	*m*M
CLL-004	B	M	UNK	1.48 6 0.55	0.56 6 0.03
CLL-005	A	M	13q and 11q deletion	0.07 6 0.03	0.49 6 0.11
CLL-006	C	F	13q deletion	2.47 6 0.39	0.49 6 0.05
CLL-017	B	M	13q and 11q deletion	0.08 6 0.02	0.17 6 0.07
CLL-024	C	F	13q deletion	8.33 6 0.29	ND
CLL-027	B	F	None	11.0 6 1.50	4.55 6 0.22
CLL-028	A	F	None	2.17 6 0.02	ND
CLL-030	B	M	13q and 11q deletion	0.80 6 0.05	ND
CLL-036	A	M	UNK	15.2 6 3.74	ND
CLL-038	A	M	UNK	5.86 6 0.58	5.63 6 0.95
MEC-1	—	—	Near-diploid karyotype with 10% polyploidy-46(44-47) , 2n - XY. t(1;6)(q22-23;p21); add(7)(q11); del(17)(p11)	5.36 6 0.94	0.22 6 0.03

B-CLL, B-cell chronic lymphocytic leukemia; ND, not determined; UNK, unknown- Not available.

cells co-cultured with MSCs (Pillozzi et al., 2011). For this purpose we tested 5 *m*M CD-160130 on either leukemic cell lines or primary samples (Fig. 7). In primary samples, $K_V11.1$ expression was evaluated by flow cytometry as in Pillozzi et al. (2011) (the mean fluorescence intensity data, MFI, are reported in Fig. 7, B and D). CD-160130 induced leukemia cell apoptosis on both suspended cells and cells cultured onto MSCs. As previously reported (Pillozzi et al., 2011), MSCs protected leukemia cells from the apoptosis induced by either chemotherapeutic drugs or CD-160130. Moreover, CD-160130 was able to overcome the MSC-induced chemoresistance. In primary samples, the proapoptotic effect of CD-160130 generally correlated with $K_V11.1$ expression.

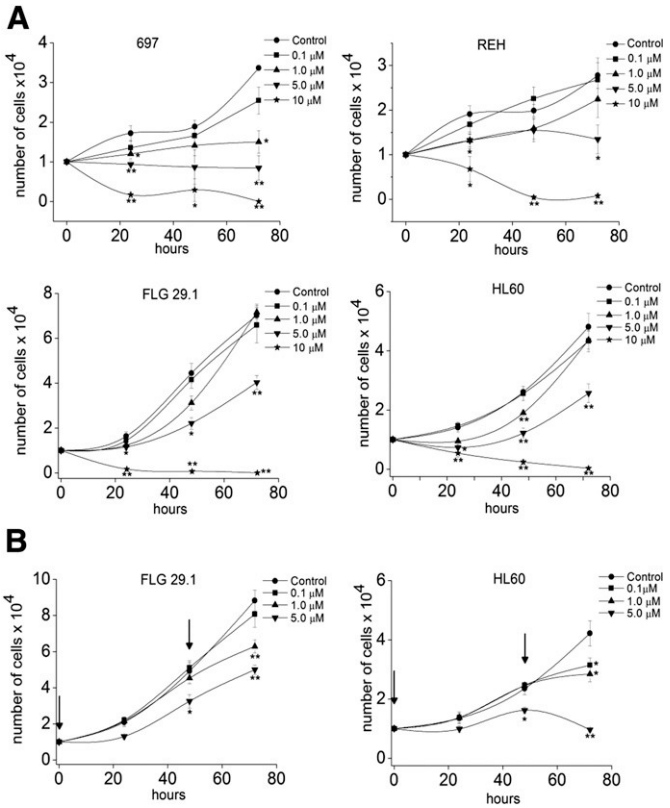

Fig. 6. CD-160130 inhibits leukemia cell proliferation. (A) Effects of CD-160130 on 697, REH, FLG 29.1, and HL60 proliferation, after a single treatment at time 0; for REH 24h P , 0.05 at both 1, 5, and 10 *m*M CD-160130; for FLG 29.1 24h P , 0.05 at 5 *m*M CD-160130. (B) Effects of CD-160130 on FLG 29.1 and HL60 proliferation, after a double treatment at time 0 and after 48 hours (arrows), given as the number of Trypan Blue negative cells (see Supplemental Material). **P , 0.01; *P , 0.05.

In NB4 leukemic cells, interaction with MSCs is known to trigger the Akt/GSK3*b* and ERK1/2/STAT3 pathways (Tabe et al., 2007). On the other hand, we previously showed that in 697 cells MSCs stimulate phosphorylation of ERK1/2 and Akt (Pillozzi et al., 2011). CD-160130 turned out to modulate both signaling pathways (Fig. 8, A and B; Supplemental Fig. 6) in these cell lines. To demonstrate that the effects of CD-160130 on cell signaling were related to its action on $K_V11.1B$, we analyzed FLG 29.1 cells treated with $K_V11.1$ siRNAs. CD-160130 significantly inhibited ERK1/2 phosphorylation after 30 and 60 minutes of treatment (Fig. 8C, left panel). Consistently, $K_V11.1$ silencing produced a significant decrease of pERK1/2, measured after 60 minutes of incubation. The addition of CD-160130 to $K_V11.1$-silenced FLG 29.1 cells did not produce any further effect on pERK1/2 (Fig. 8C, right panel).

Effect of CD-160130 on Leukemia In Vivo. Finally, we evaluated the efficacy of CD-160130 on a preclinical leukemia model, consisting of severe combined immunodeficiency mice injected i.p. with HL60 cells transfected with the firefly luciferase gene (HL60-luc2 cells). Mice were monitored weekly, and the luciferase activity signal was quantified. The overall survival was also measured. The results are reported in Fig. 9. The administration schedules were: (1) 1 mg/Kg, daily for 14 days; (2) 10 mg/Kg, daily for 14 days; and (3) 10 mg/kg, daily for 7 days, followed by 20 mg/kg for 7 days. In all cases, CD-160130 was administered by mouth starting from day 5 (e.g., when leukemia cells started to engraft, Fig. 9A). The rationale for such a treatment schedule relied on biodistribution data (Fig. 9D) showing that (1) administration of 10 mg/Kg gave rise to a peak plasma concentration of around 4 ng/ml (11 nM) after 2 hours; (2) 20 mg/Kg gave rise to a peak plasma concentration of around 12 ng/ml (31 nM) between 2 and 4 hours; and (3) 1 mg/Kg was not effective. The details and statistics are given in Supplemental Table 4. The effects of CD-160130 were compared with those observed in mice treated with Ora-Plus (Paddock Laboratories) or with the chemotherapeutic drug cytarabine. CD-160130 effectively reduced the leukemia burden in a dose-dependent manner (Fig. 9B). In particular, at

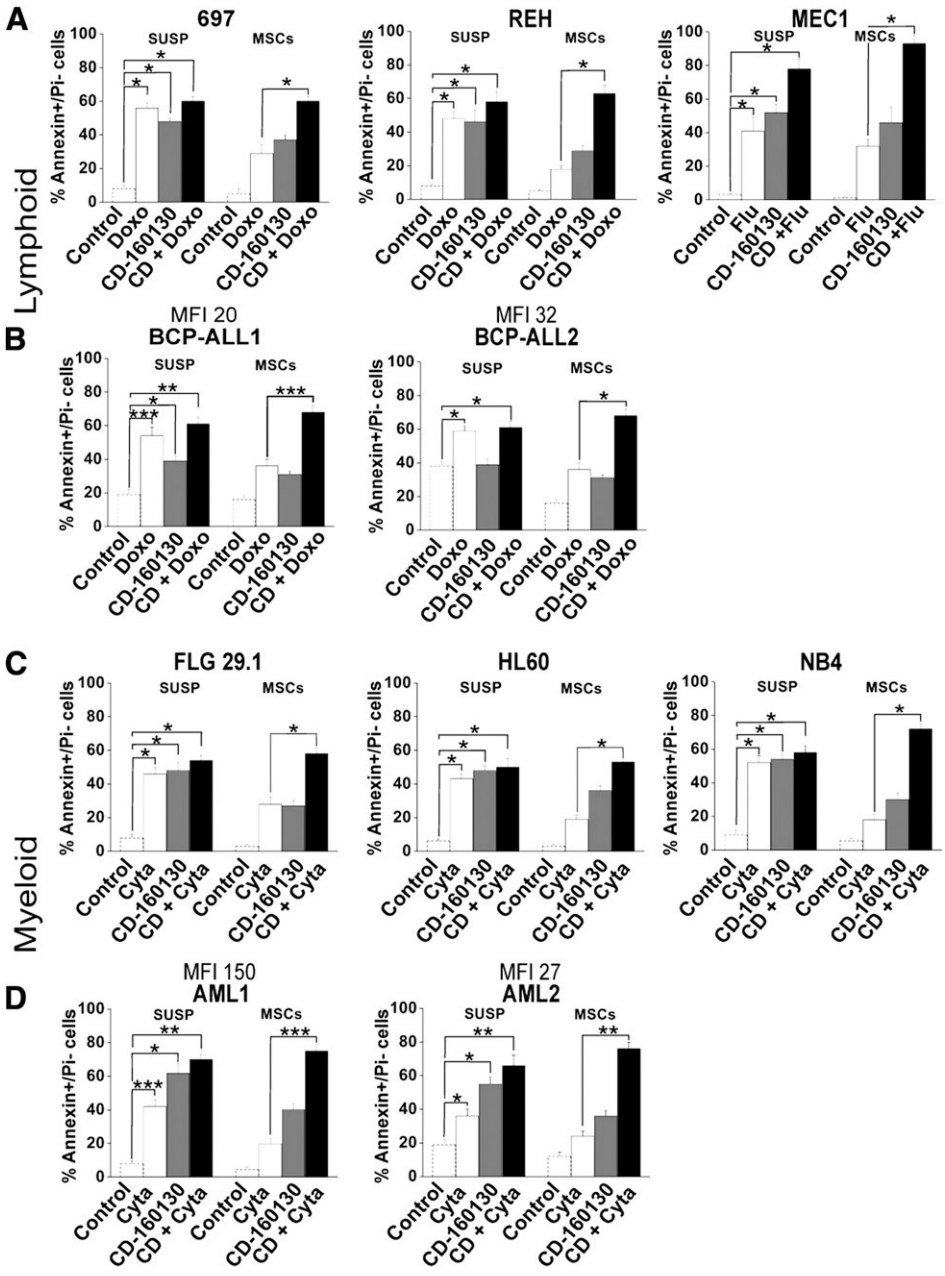

Fig. 7. CD-160130 overcomes MSC-induced chemoresistance by inducing apoptosis. 697, REH, MEC1 cell line (A) and two representative BCP-ALL primary samples (B) were cultured with or without MSCs (suspension) and treated with LD_{50} doses of either fludarabine (0.22 *m*M), doxorubicin (0.1 *m*g/mL), or CD-160130 (5 *m*M) for 48 hours. The effects of the treatment were evaluated on early apoptosis (annexin + propidium iodide 2 cells). $K_V11.1$ expression in primary samples, evaluated by flow cytometry using the anti- $K_V11.1$ antibody, is reported as the mean fluorescence index (MFI). The MFI of BCP-ALL1 was 20, while the MFI for BCP-ALL2 was 32. FLG 29.1, HL60, and NB4 cell lines (C) and two representative AML primary samples (D) were cultured with or without MSCs (suspension) and treated with LD_{50} doses of either cytarabine (45 nM) or CD-160130 (5 *m*M) for 48 hours. The MFI of AML1 was 150, while the MFI for AML2 was 27. The values of the untreated controls are reported as dotted bars in each graph. Statistical analysis for the data in panels (A) and (C) was carried out with the Mann-Whitney test; statistical analysis for the data in panels (B) and (D) was carried out with the Student's *t* test (**P* , 0.05; ***P* , 0.01; ****P* , 0.001).

10 mg/kg the leukemia progression was comparable to, or even slower than, that occurring in the mice group treated with cytarabine (Fig. 9, A and B). No improvement was observed by increasing the dosage of the drug to 20 mg/Kg. The treatment at 10 mg/kg also improved mice survival, with survival times longer than those obtained with cytarabine (Fig. 9C).

Effect of CD-160130 on Cardiac Physiology. One of the major hindrances for considering $K_V11.1$ as a therapeutic target in oncology is the cardiac side effects that many $K_V11.1$ blockers exert (Redfern et al., 2003; Raschi et al., 2008). Such effects mainly consist of a lengthening of the cardiac AP (cAP), which is reflected in the lengthening of the ECG QT interval. First, we registered the ECG in mice treated with 10 or 20 mg/kg CD-160130 (Fig. 9E; Supplemental Table 5). No alterations of either the heart rate or the compensated QT interval were observed. The compensated QT interval was also not affected after 2 weeks of chronic daily administration (Fig. 9F; Supplemental Table 6).

Next, we tested the QT liability of CD-160130 by measuring its effects on the cAP stimulated in acutely isolated left ventricular guinea pig cardiomyocytes recorded at physiologically relevant temperatures (i.e., at 37°C). Guinea pig myocytes were chosen because (unlike those of smaller rodents) they exhibit cAP features similar to those observed in humans, i.e., a long depolarized cAP plateau and heavy reliance on delayed rectifier potassium currents. CD-160130 failed to lengthen the AP duration (Fig. 10A). In particular, 1 *m*M CD-160130 shortened AP duration at 90% repolarization by less than 1 millisecond (20.8 6 2.3 milliseconds, *n* 5 7), while 10 *m*M CD-160130 lengthened AP duration at 90% repolarization by 2.7 6 7.4 milliseconds (*n* 5 6). Additionally, we analyzed the effects of CD-160130 on ECG parameters of anesthetized guinea pigs, an accepted in vivo model for the evaluation of

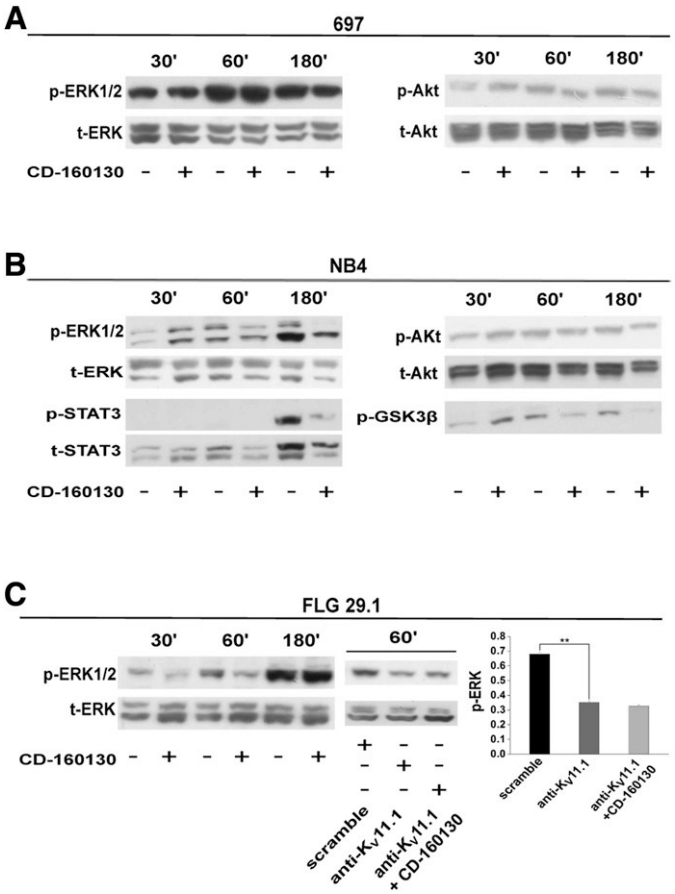

Fig. 8. Effect of CD-160130 on cell signaling. (A) Western blot analysis of the protein levels of p-ERK1/2$^{Thr202/Tyr204}$ (42/44 KDa) and p-Akt^{Thr308} (60 KDa) in 697 cells after co-culture for 30, 60, and 180 minutes with MSCs in the absence or presence of CD-160130. The membranes were then reprobed with an anti-ERK1/2 or anti-Akt antibody. (B) p-ERK1/2$^{Thr202/Tyr204}$ (42/44 KDa), p-STAT3^{Tyr705} (80 KDa), p-Akt^{Thr308} (60 KDa), and p-GSK3b^{Ser9} (47 KDa) in NB4 cells after co-culture for 30, 60, and 180 minutes with MSCs in the absence or presence of CD-160130. The membranes were then reprobed with an anti-ERK1/2, anti-STAT3, or anti-Akt antibody. Experiments shown are representative of at least two independent experiments. (C) Western blot analysis of the protein levels of p-ERK1/2$^{Thr202/Tyr204}$ (42/44 KDa) in control FLG 29.1 cells after co-culture for 30, 60, and 180 minutes with MSCs in the absence or presence of CD-160130 (left); p-ERK1/2$^{Thr202/Tyr204}$ (42/44 KDa) protein levels in transfected with siRNA scramble and siRNA anti-K_V11.1 after co-culture for 60 minutes with MSCs in the absence or presence of CD-160130 (right). Bars show the densitometric analysis of the siRNA-treated FLG 29.1. Values in the *Y*-axis are reported as the ratio between phosphorylated and total protein.

drug cardiotoxicity (Morissette et al., 2013). In these experiments, we injected CD-160130 i.v. at 10 mg/kg in a proper vehicle. CD-160130 did not produce any significant QT prolongation (Fig. 10B) up to 15 minutes after administration. The raw data, relative to either CD-160130, sotalol, or the vehicles, up to 60 minutes of infusion, are given in Supplemental Table 7. As a positive control, we used sotalol (3 mg/Kg, i.v.), which increased the compensated QT interval by approximately 10%, as expected (Hauser et al., 2005).

Discussion

CD-160130 is a pyrimido-indole compound, initially developed as a PDE-4 inhibitor with the aim of inducing leukemia killing. In fact, micromolar concentration of CD-160130 reduced cell viability both in leukemia cell lines and primary leukemia samples (Tables 1–4). In the latter, the effect of CD-160130 was more evident in the harder to treat cases, such as T-ALL and double-deleted CLL. However, cytotoxicity turned out to be not a result of PDE-4 inhibiting (Fig. 1; Supplemental Table 1). An alternative hypothesis is that the antileukemic effect of CD-160130 depends on K_V11.1 inhibition, as suggested by the effect we observed with anti-K_V11.1 siRNAs. In agreement with this notion, CD-160130 turned out to block K_V11.1 channels. Also, CD-160130 displayed properties of channel block considerably different from those shown by classic K_V11.1 blockers, such as the type III antiarrhythmics. In fact, CD-160130 inhibited K_V11.1B with a 7.6-fold higher potency, compared with K_V11.1A, and strongly inhibited K_V11.1 almost independently of Phe656, which is the main binding site of type III antiarrhythmics, such as E4031. The fact that CD- 160130 is somewhat less efficacious in blocking F656A K_V11.1 compared with the wild-type channel probably depends on alterations produced on the pore structure by the nonconservative F656A substitution. Nonetheless, the striking difference between the actions of E4031 and CD-160130 on F656A K_V11.1 suggests that either Phe656 makes a minor contribution to the inhibitory effect of CD-160130 or the F656A mutation has an allosteric effect on CD-160130 binding.

Successful treatment of acute and chronic leukemias is often impeded by the development of resistance to cytotoxic drugs, either at the initial presentation or following relapse (Pui and Evans, 2006). We showed in ALL that the chemoresistance triggered by MSCs in the BM microenvironment is overcome by blocking K_V11.1 channels (Pillozzi et al., 2011). In this paper, we showed that CD-160130 strongly inhibited the leukemia burden in an AML mouse model and significantly prolonged mice survival; the response was even better than cytarabine, a classic chemotherapeutic drug used in AML. The effect was evident with a schedule of daily oral administrations of 10 mg/Kg, which corresponds to plasma-free concentrations of approximately 12 nM. This concentration is lower than the IC_{50} for K_V11.1 obtained from patch-clamp experiments. For CD-160130, a plasma-free concentration of 12 nM would block approximately 15% of the channels if they were activated by the acute application protocol used in Fig. 4A. We hypothesize that, considering also the slow kinetics of CD-160130 unbinding, the sustained presence of the drug in plasma produces cumulative inhibition by progressively removing increasing fractions of K_V11.1 channels from the steady-state open-close equilibrium, thus making them unavailable to open. Consistently, when we tested the effects of CD-160130 on leukemia cell proliferation in vitro, we observed that when the drug was applied only once at the lower concentrations, after an initial block (lasting about 24 hours), FLG 29.1 and HL60 cells started to proliferate again. However, the effect was potentiated by subsequent readditions, e.g., when CD-160130 was reapplied to the cells after 48 hours, the inhibition of cell proliferation was sustained (for FLG 29.1, Fig. 6B) or complete (for HL60, Fig. 6B). In these conditions, even 0.1 *m*M produced significant reduction of cell proliferation. This is also in agreement with recent results by Pier et al. (2014) showing that nonsaturating concentrations of hERG1 blockers need to be applied for long periods of time to fully produce their antitransformation effects. Although different leukemia models and different administration schedules (e.g., twice per day) could be tested, our in vivo data indicate that CD-160130 is

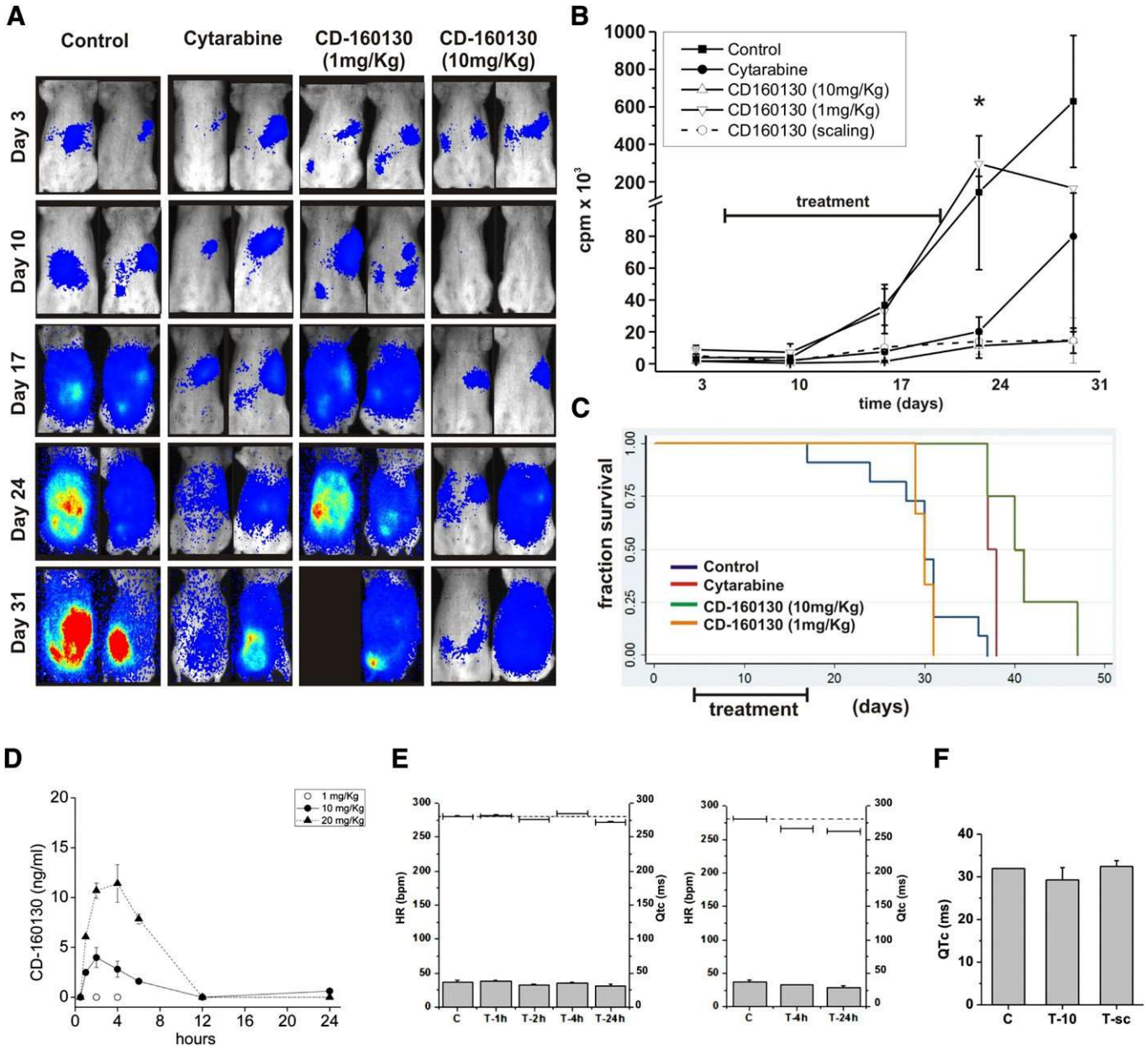

Fig. 9. CD-160130 reduces leukemia burden in a preclinical leukemia model. (A) Severe combined immunodeficiency mice were injected with HL60-luc2 cell line (5 ×10⁶ cells i.p.). Starting from day 5, animals were treated daily for 14 consecutive days with Ora-Plus (Paddock Laboratories; control, $n = 9$), cytarabine (6.25 mg/Kg, $n = 4$); CD-160130 (1 mg/Kg, $n = 3$); and CD-160130 (10 mg/Kg, $n = 4$). Images were acquired with Photo Acquisition software (Biospace Laboratory, Paris, France) and processed with M3 Vision software (Biospace Laboratory). Two representative animals for each treatment condition are shown. (B) Counts per minutes (cpm) reported as the time scale. The cpm values from a separate experiment (called scaling) are also included (dashed line). The scaling group received CD-160130 daily, from day 5 to 11 at the dose of 10 mg/Kg and from day 12 to 18 at the dose of 20 mg/Kg. At day 24, the signal relative to the CD-160130 (10 mg/kg) group was significantly reduced from the control group (P , 0.05). (C) Survival curves of each experimental group, estimated by Kaplan and Meier analysis. (D) CD-160130 plasma distribution. Pharmacokinetics of CD-160130 (ng/ml) analyzed in the plasma of CD1 mice after a single oral administration (10 or 20 mg/kg). Blood samples were collected at different time points (at least $n = 2$) and analyzed by high-performance liquid chromatography (see Supplemental Material). Two more mice were administered with a single dose of CD-160130 (1 mg/kg). Blood was collected 2 and 4 hours postoral gavage, corresponding to the higher registered values of plasma concentration for the doses previously tested. In both cases CD-160130 plasma concentration was undetectable (open circles). (E) ECG parameters of CD-1 mice at different time points after acute administration of CD-160130 (10 mg/Kg, left panel) and CD-160130 (20 mg/Kg, right panel): ECG results consisting of heart rate (HR, dashed lines) and HR compensated QT (QTc) intervals are shown (bars). The QTc interval was calculated by applying Bazett's formula (Mitchell et al., 1998): QTc ¼ QT= ðRR=100Þ interval. (F) ECG parameters in mice after chronic administration of CD-160130 (T-10, 10 mg/Kg for 14 consecutive days or T-sc, 10 mg/Kg for seven days followed by 20 mg/Kg for another seven days) in CD-1 mice: ECG results consisting of QTc intervals are shown. Experimental details are widely described in the Supplemental Material.

even more effective in its antileukemic action after repeated administrations.

On the whole, Kv11.1 would seem an attractive target for antineoplastic therapy, particularly in leukemias. However, Kv11.1 is normally considered as an antitarget, since blocking Kv11.1 can lead to serious cardiac side effects (Redfern et al., 2003; Raschi et al., 2008). The present results suggest that CD-160130 could be a first-in-class Kv11.1 channel

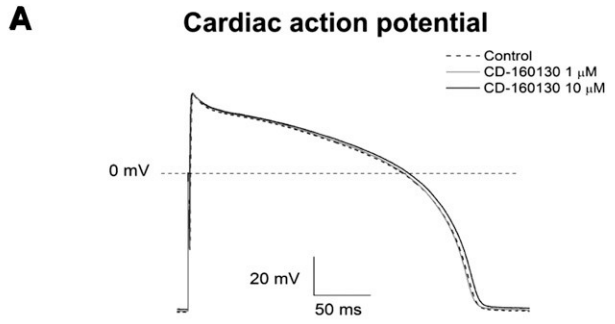

B

ECG parameters

CD-160130 (n=5) 10mg/kg	QT ± SEM (ms)	HR ± SEM (beat/min)	QTc ± SEM	ΔQTc (% vs Pre-drug)
Pre-drug	129.0 ± 4.2	237.1 ± 3.4	305.1 ± 7.5	-
0 min	131.4 ± 5.4	241.1 ± 5.2	308.4 ± 7.4	1.1 ± 3.5
5 min	127.5 ± 7.0	249.1 ± 1.1	298.8 ± 12.9	-2.1 ± 4.9
10 min	129.0 ± 5.8	240.5 ± 3.4	300.9 ± 11.2	-1.4 ± 4.4
15 min	128.0 ± 6.7	240.5 ± 2.8	298.6 ± 11.8	-2.2 ± 4.6
Sotalol (n=5) 3mg/kg	QT ± SEM (ms)	HR ± SEM (beat/min)	QTc ± SEM	ΔQTc (% vs Pre-drug)
Pre-drug	115.4 ± 3.6	240.3 ± 3.7	276.4 ± 6.8	-
0 min	115.4 ± 3.8	240.4 ± 5.1	273.7 ± 6.7	-1.0 ± 3.4
5 min	132.7 ± 4.0	240.4 ± 1.2	301.1 ± 6.2	8.9 ± 3.5
10 min	135.3 ± 4.2	235.0 ± 3.1	304.3 ± 6.1	10.1 ± 3.5
15 min	133.0 ± 5.8	232.2 ± 4.5	299.5 ± 8.0	8.4 ± 3.9

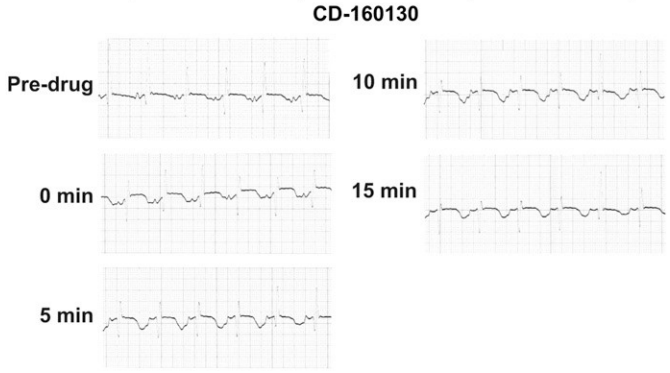

Fig. 10. CD-160130 effects on guinea pig APs of ventricular cardiomyocytes and ECG parameters. (A) Representative APs elicited in isolated ventricular cardiomyocytes of guinea pig, in the presence or in the absence of 1 and 10 *m*M CD-160130. Under all conditions, 20 APs were averaged and used to measure the AP duration at 90% repolarization values. (B) ECG registrations were performed in five anesthetized male Dunkin-Hartley guinea pigs after i.v. administration of CD-160130 (10 mg/kg, suspended in 5% Kolliphor in 0.9% NaCl solution) or in five anesthetized male Dunkin-Hartley guinea pigs after i.v. administration of sotalol (3 mg/Kg). ECGs were performed at several time points starting with a registration pre-drug administration and lasting for at least 1 hour. At least eight ECG traces were analyzed for each time point of each monitored guinea pig. QT intervals, heart rate (HR), and compensated QT (QTc) interval calculations for the following time points were reported: pre-drug, 0, 5, 10, and 15 minutes after CD-160130 injection. QTc was calculated with Bazett's formula as in Hauser et al. (2005) for the anesthetized guinea pig. QTc ¼ QT= RR. On the bottom, representative ECG traces were reported at the different time points.

inhibitor appropriate for the treatment of leukemias since it overcame the chemoresistance induced in vitro by cell interaction with MSC and tightly controlled the leukemia burden in vivo, but without significant QT liability in guinea pigs. One possible explanation for these results is that because leukemia cells overexpress the Kv11.1B isoform of Kv11.1 (Crociani et al., 2003; Pillozzi et al., 2007, 2014), compared with cardiac cells (Pond et al., 2000, Jones et al., 2004; Sale et al., 2008; Larsen and Olesen 2010), the higher efficacy of CD-160130 on Kv11.1B could decrease the harmful effect on cardiac cells, without impairing the antileukemic effect. Another possibility is that the lack of effect of CD-160130 on the QT interval depends on the fact that this compound acts with a different mechanism from the classic class III antiarrythmic drugs. At the present stage, we cannot discriminate these mechanisms. Nonetheless, the characterization of CD-160130 opens the way to the development of compounds with a higher selectivity for the different Kv11.1 isoforms, accompanied by inhibitory action on the chemotherapy resistant leukemia forms and negligible QT liability.

Acknowledgments

The authors thank Dr. H. Witchel for sharing the Kv11.1 F656A vector, Dr. GN. Tseng for sharing the G628C:S631C vector, and Dr. P.A. Bernabei for contributing to the analysis of the clonogenic assay.

Authorship Contributions

Participated in research design: Arcangeli, Becchetti, Gasparoli, D'Amico, Masselli, Pillozzi, Mitcheson, Basso.

Conducted experiments: Gasparoli, D'Amico, Masselli, Caves, Khuwaileh, Pillozzi, Mitcheson, Mugridge, Pratesi

Contributed new reagents or analytic tools: Tiedke, Mugridge.

Performed data analysis: Arcangeli, Becchetti. Gasparoli, D'Amico, Masselli, Pillozzi, Pratesi, Mitcheson.

Wrote or contributed to the writing of the manuscript: Arcangeli, Becchetti, Gasparoli, D'Amico, Masselli, Pillozzi, Mugridge, Mitcheson.

References

Arcangeli A (2005) Expression and role of hERG channels in cancer cells. *Novartis Found Symp* 266:225–232; discussion 232–224.

Arcangeli A, Crociani O, Lastraioli E, Masi A, Pillozzi S, and Becchetti A (2009) Targeting ion channels in cancer: A novel frontier in antineoplastic therapy. *Curr Med Chem* 16:66–93.

Arcangeli A, Pillozzi S, and Becchetti A (2012) Targeting ion channels in leukemias: A new challenge for treatment. *Curr Med Chem* 19:683–696.

Crociani O, Guasti L, Balzi M, Becchetti A, Wanke E, Olivotto M, Wymore RS, and Arcangeli A (2003) Cell cycle-dependent expression of HERG1 and HERG1B isoforms in tumor cells. *J Biol Chem* 278:2947–2955.

Crociani O, Zanieri F, Pillozzi S, Lastraioli E, Stefanini M, Fiore A, Fortunato A, D'Amico M, Masselli M, and De Lorenzo E et al. (2013) hERG1 channels modulate integrin signaling to trigger angiogenesis and tumor progression in colorectal cancer. *Sci Rep* 3:3308.

Dalton WT, Jr, Ahearn MJ, McCredie KB, Freireich EJ, Stass SA, and Trujillo JM (1988) HL-60 cell line was derived from a patient with FAB-M2 andnot FAB-M3. *Blood* 71:242–247.

De Bruin ML, Pettersson M, Meyboom RH, Hoes AW, and Leufkens HG (2005) Anti-HERG activity and the risk of drug-induced arrhythmias and sudden death. *Eur Heart J* 26:590–597.

Faravelli L, Arcangeli A, Olivotto M, and Wanke E (1996) A HERG-like K^1 channel in rat F-11 DRG cell line: Pharmacological identification and biophysical characterization. *J Physiol* 496:13–23.

Guasti L, Crociani O, Redaelli E, Pillozzi S, Polvani S, Masselli M, Mello T, Galli A, Amedei A, and Wymore RS et al. (2008) Identification of a posttranslational mechanism for the regulation of hERG1 K^1 channel expression and hERG1 current density in tumor cells. *Mol Cell Biol* 28:5043–5060.

Hauser DS, Stade M, Schmidt A, and Hanauer G (2005) Cardiovascular parameters in anaesthetized guinea pigs: A safety pharmacology screening model. *J Pharmacol Toxicol Methods* 52:106–114.

Jehle J, Schweizer PA, Katus HA, and Thomas D (2011) Novel roles for hERG K^1 channels in cell proliferation and apoptosis. *Cell Death Dis* 2:e193.

Jones EM, Roti Roti EC, Wang J, Delfosse SA, and Robertson GA (2004) Cardiac I_{Kr} channels minimally comprise hERG 1a and 1b subunits. *J Biol Chem* 279: 44690–44694.

Kamiya K, Niwa R, Mitcheson JS, and Sanguinetti MC (2006) Molecular determinants of HERG channel block. *Mol Pharmacol* 69:1709–1716.

Kim DH and Lerner A (1998) Type 4 cyclic adenosine monophosphate phosphodiesterase as a therapeutic target in chronic lymphocytic leukemia. *Blood* 92: 2484–2494.

Larsen AP and Olesen SP (2010) Differential expression of hERG1 channel isoforms reproduces properties of native I_{Kr} and modulates cardiac action potential characteristics. *PLoS ONE* 5:e9021.

Lees-Miller JP, Kondo C, Wang L, and Duff HJ (1997) Electrophysiological characterization of an alternatively processed ERG K^1 channel in mouse and human hearts. *Circ Res* 81:719–726.

Lerner A and Epstein PM (2006) Cyclic nucleotide phosphodiesterases as targets for treatment of haematological malignancies. *Biochem J* 393:21–41.

Levesque MC, O'Loughlin CW, and Weinberg JB (2001) Use of serum-free media to minimize apoptosis of chronic lymphocytic leukemia cells during in vitro culture. *Leukemia* 15:1305–1307.

Masi A, Becchetti A, Restano-Cassulini R, Polvani S, Hofmann G, Buccoliero AM, Paglierani M, Pollo B, Taddei GL, Gallina P et al. (2005) hERG1 channels are overexpressed in glioblastoma multiforme and modulate VEGF secretion in glioblastoma cell lines. *Br J Cancer* 93:781–92.

Mitchell GF, Jeron A, and Koren G (1998) Measurement of heart rate and Q-T interval in the conscious mouse. *Am J Physiol* 274:H747–H751.

Morais Cabral JH, Lee A, Cohen SL, Chait BT, Li M, and Mackinnon R (1998) Crystal structure and functional analysis of the HERG potassium channel N terminus: A eukaryotic PAS domain. *Cell* 95:649–655.

Morissette P, Nishida M, Trepakova E, Imredy J, Lagrutta A, Chaves A, Hoagland K, Hoe CM, Zrada MM, Travis JJ et al. (2013) The anesthetized guinea pig: an effective early cardiovascular derisking and lead optimization model *J Pharmacol Toxicol Methods* 68:137–49.

Pelliccia F, Ubertini V, and Bosco N (2012) The importance of molecular cytogenetic analysis prior to using cell lines in research: The case of the KG-1a leukemia cell line. *Oncol Lett* 4:237–240.

Pier DM, Shehatou GS, Giblett S, Pullar CE, Trezise DJ, Pritchard CA, Challiss RA, and Mitcheson JS (2014) Long-term channel block is required to inhibit cellular transformation by human ether-à-go-go-related gene (hERG1) potassium channels. *Mol Pharmacol* 86:211–221.

Pillozzi S, Accordi B, Rebora P, Serafin V, Valsecchi MG, Basso G, and Arcangeli A (2014) Differential expression of *hERG1A* and *hERG1B* genes in pediatric acute lymphoblastic leukemia identifies different prognostic subgroups. *Leukemia* 28: 1352–1355.

Pillozzi S, Brizzi MF, Balzi M, Crociani O, Cherubini A, Guasti L, Bartolozzi B, Becchetti A, Wanke E, and Bernabei PA et al. (2002) HERG potassium channels are constitutively expressed in primary human acute myeloid leukemias and regulate cell proliferation of normal and leukemic hemopoietic progenitors. *Leukemia* 16:1791–1798.

Pillozzi S, Brizzi MF, Bernabei PA, Bartolozzi B, Caporale R, Basile V, Boddi V, Pegoraro L, Becchetti A, and Arcangeli A (2007) VEGFR-1 (FLT-1), b_i integrin, and hERG K^1 channel for a macromolecular signaling complex in acute myeloid leukemia: Role in cell migration and clinical outcome. *Blood* 110:1238–1250.

Pillozzi S, Masselli M, De Lorenzo E, Accordi B, Cilia E, Crociani O, Amedei A, Veltroni M, D'Amico M, and Basso G et al. (2011) Chemotherapy resistance in acute lymphoblastic leukemia requires hERG1 channels and is overcome by hERG1 blockers. *Blood* 117:902–914.

Pond AL, Scheve BK, Benedict AT, Petrecca K, Van Wagoner DR, Shrier A, and Nerbonne JM (2000) Expression of distinct ERG proteins in rat, mouse, and human heart. Relation to functional I_{Kr} channels. *J Biol Chem* 275:5997–6006.

Pui CH and Evans WE (2006) Treatment of acute lymphoblastic leukemia. *N Engl J Med* 354:166–178.

Raschi E, Vasina V, Poluzzi E, and De Ponti F (2008) The hERG K^1 channel: Target and antitarget strategies in drug development. *Pharmacol Res* 57:181–195.

Redfern WS, Carlsson L, Davis AS, Lynch WG, MacKenzie I, Palethorpe S, Siegl PK, Strang I, Sullivan AT, and Wallis R et al. (2003) Relationships between preclinical cardiac electrophysiology, clinical QT interval prolongation and torsade de pointes for a broad range of drugs: Evidence for a provisional safety margin in drug development. *Cardiovasc Res* 58:32–45.

Reichelt C, Schulze A, Daghish M, Ludwig FA, Heinicke J, Herrmann K, Schuster M, Letschert S, Mugridge K, and DeAngelo J (2014) inventors, The Medicines Company (Leipzig) Gmbh, assignee. Substituted 5H-pyrimido[5,4-B]indoles, method for the production thereof and use thereof for treating non-solid malignant tumors of the blood-producing system. Patent 8664233, 2014 Mar 4.

Sale H, Wang J, O'Hara TJ, Tester DJ, Phartiyal P, He JQ, Rudy Y, Ackerman MJ, and Robertson GA (2008) Physiological properties of hERG 1a/1b heteromeric currents and a hERG 1b-specific mutation associated with long-QT syndrome. *Circ Res* 103:e81–e95.

Sanguinetti MC, Jiang C, Curran ME, and Keating MT (1995) A mechanistic link between an inherited and an acquired cardiac arrhythmia: *HERG* encodes the I_{Kr} potassium channel. *Cell* 81:299–307.

Sanguinetti MC and Mitcheson JS (2005) Predicting drug-hERG channel interactions that cause acquired long QT syndrome. *Trends Pharmacol Sci* 26:119–124.

Sanguinetti MC and Tristani-Firouzi M (2006) hERG potassium channels and cardiac arrhythmia. *Nature* 440:463–469.

Sankaranarayanan A, Raman G, Busch C, Schultz T, Zimin PI, Hoyer J, Köhler R, and Wulff H (2009) Naphtho[1,2-*d*]thiazol-2-ylamine (SKA-31), a new activator of KCa2 and KCa3.1 potassium channels, potentiates the endothelium-derived hyperpolarizing factor response and lowers blood pressure. *Mol Pharmacol* 75: 281–295.

Smith GA, Tsui HW, Newell EW, Jiang X, Zhu XP, Tsui FW, and Schlichter LC (2002) Functional up-regulation of HERG K^1 channels in neoplastic hematopoietic cells. *J Biol Chem* 277:18528–18534.

Spector PS, Curran ME, Zou A, Keating MT, and Sanguinetti MC (1996) Fast inactivation causes rectification of the I_{Kr} channel. *J Gen Physiol* 107:611–619.

Tabe Y, Jin L, Tsutsumi-Ishii Y, Xu Y, McQueen T, Priebe W, Mills GB, Ohsaka A, Nagaoka I, and Andreeff M et al. (2007) Activation of integrin-linked kinase is a critical prosurvival pathway induced in leukemic cells by bone marrow-derived stromal cells. *Cancer Res* 67:684–694.

Trudeau MC, Warmke JW, Ganetzky B, and Robertson GA (1995) HERG, a human inward rectifier in the voltage-gated potassium channel family. *Science* 269:92–95.

Tseng GN (2001) I_{Kr}: The hERG channel. *J Mol Cell Cardiol* 33:835–849.

Viskin S (1999) Long QT syndromes and torsade de pointes. *Lancet* 354:1625–1633.

Weinberg JB, Jiang N, Volkheimer AD, Chen Y, Bond KM, Moore JO, Gockerman JP, Diehl LF, de Castro CM, and Rizzieri DA et al. (2007) Cytotoxicity of the type 4 phosphodiesterase inhibitor CD160130 for freshly isolated human CLL cells in vitro. *Blood* 110:920a.

Zimin PI, Garic B, Bodendiek SB, Mahieux C, Wulff H, and Zhorov BS (2010) Potassium channel block by a tripartite complex of two cationophilic ligands and a potassium ion. *Mol Pharmacol* 78:588–599.

Address correspondence to: Annarosa Arcangeli, Department of Experimental and Clinical Medicine, University of Firenze, Viale G.B. Morgagni, 50, 50134 Firenze, Italy. E-mail: annarosa.arcangeli@unifi.it